Donor impurity on-center and off-center in multilayered quantum wires in the presence of magnetic field

Cheng-Ying Hsieh[a)]
Deh Yu College of Nursing and Management, Keelung 203, Taiwan, Republic of China

(Received 26 November 2001; accepted for publication 27 March 2002)

The binding energies of a hydrogenic impurity located at the center and off-center of a multilayered quantum wire (MLQW) in the presence of magnetic field are studied within the framework of the effective-mass approximation. The MLQW consists of a GaAs core wire coated by a $Al_xGa_{1-x}As$ cylindrical shell and embedded in the bulk $Al_yGa_{1-y}As$. A variational trial wave function is proposed. It is found for a small wire radius that the ground state binding energy of a hydrogenic impurity located at the center of a MLQW behaves very differently from that of a single-layered quantum wire (SLQW). The calculation shows that the binding energy depends on the potential profiles, potential barrier height, impurity position, shell thickness, magnetic field, and the difference between the Al concentration contained in the shell and bulk regions. Our trial function is also able to reproduce the binding energies of a hydrogenic impurity located at the center of a SLQW, good agreement with the previous results is obtained. © *2002 American Institute of Physics.* [DOI: 10.1063/1.1480121]

I. INTRODUCTION

Semiconductor heterostructures are shown to provide a large number of interesting physical phenomena and important practical applications, such as in photodetector and optoelectronical devices. The design of such devices depends strongly on the spectral range of interest. On the other hand, the desired energy range may be obtained and controlled by various mechanisms including doping, application of external fields such as magnetic, electric and laser, and also by choosing appropriate potential profiles of the systems.

Since the pioneer work of Bastard[1] in the study of the binding energy of a hydrogenic impurity within an infinite potential-well structure, many theoretical works have been devoted to the study of the properties of impurity states in various confining systems.[1–18] The binding energy of the ground state of a hydrogenic impurity E_b in D dimension is given by[19] $E_b=[2/(D-1)]^2$ Ry, where Ry is the effective Rydberg and can be expressed by $\mu e^4/2\hbar^2\epsilon^2$, where μ and ϵ are the electronic effective mass and the dielectric constant. The physical properties of electrons in quantum wires are very different from those in the bulk system. As a consequence of the confinement, energy levels are discrete. The existence of these atomic-like states may be utilized in a future laser where laser properties can be tailored by proper choices of well and barrier materials as well as the size and shape of the wire.[20,21] The change in impurity binding energies due to the confinement effect has been observed in photoluminescence[7,22–24] and Raman-scattering[25,26] experiments on the impurities in the quantum wells. Recently, $GaAs-Al_xGa_{1-x}As$ structures have been the subject of recent research for the following technological reasons:[27] (1) GaAs and $Al_xGa_{1-x}As$ both possess a direct-gap band structure, (2) single-crystal heterostructures of GaAs and $Al_xGa_{1-x}As$ are possible because the lattice constants of GaAs and $Al_xGa_{1-x}As$ are nearly identical, so that they are closely lattice matched, and, therefore, (3) abrupt spatial transitions in the energy gap are possible. However, in all of previous calculations, it has been assumed that the $Al_xGa_{1-x}As$ layers are thick enough to confine the wave functions so that they do not leak out of the wells. But superlattices were made with layer thickness ranging from a few monolayers to about 400 Å. And most attention has been focused on systems with aluminum concentration x of $Al_xGa_{1-x}As$ less than 0.45. In this concentration range, the band gap is direct at the Γ point. The spreading of the impurity envelope wave functions depends on the potential barrier height as well as the barrier thickness. Thus, the previous calculations with single-layered approximation are not adequate for thin supperlattices, or even for moderately thick superlattices but with small aluminum concentration.

Chaudhuri[28] considered a three quantum well system in his variational calculation for the ground-state energy of the donor electron with respect to the lowest subband level. Lane *et al.*[29] calculated the binding energies and probability distributions of shallow donor states in a multiple-well $Al_xGa_{1-x}As$ heterostructure. Many authors[30–33] used colloidal chemistry techniques and wet chemistry to prepare the CdS/HgS/CdS multiple well in which a shell of HgS is embedded in a CdS quantum dot, forming a ''quantum-dot quantum well'' (QDQW). The homogeneous absorption and fluorescence spectra of QDQW were investigated. Numerous studies on organic light-emitting diodes have used these structures as the emitting and charge transport species.[34–36] Recently, Hsieh and Chuu calculated the state energies of an on-center hydrogenic impurity in a multilayered quantum dot and a multilayered quantum wire.[37–40]

The behavior of energy levels of shallow nature impurity states in the low dimensional quantum systems in the pres-

a)Electronic mail: hsieh@ems.dyc.edu.tw

ence of a magnetic field have been investigated in several papers.[41–56] The application of the magnetic field modifies the symmetry of the impurity states as well as the nature of the wave functions, and finally, leads to a more complicated change of the binding energy and the other properties of these impurity energy levels. The study of the behavior of shallow impurity states in the low dimensional system in the presence of a magnetic filed will lead to a better understanding of their electronic and optical properties.

In this work, we calculate the ground state binding energy of the hydrogenic impurity located at the center and off center of a multilayered quantum wire in a constant magnetic field applied parallel to the wire axis by using the effective-mass approximation. Our system is constructed as a core wire made of GaAs surrounded by a cylindrical shell of $Al_xGa_{1-x}As$ and then embedded in the bulk of $Al_yGa_{1-y}As$. The barrier height V between GaAs and $Al_xGa_{1-x}As$ can be obtained[57] as $0.8729x$ eV from a fixed ratio $Q=0.7$ of the band-gap discontinuity $\Delta E_g=1.247x$ eV. In this article, the effective atomic units are used so that all energies are measured in the units of the effective Rydberg (Ry) and all distances are measured in the units of effective Bohr radius (a_0^*). The effective Bohr radius a_0^* can be expressed by $\epsilon\hbar^2/\mu e^2$, where μ and ϵ are the electronic effective mass and the dielectric constant of GaAs material which are equal to $0.067m_e$ and 13.18, respectively. And Ry and a_0^* equal to 5.2 meV and 104 Å, respectively. In this work, the effective-mass difference between GaAs and $Al_xGa_{1-x}As$ material has been ignored. The polarization and image charge effects may be significant in the multilayered system if there is a large dielectric discontinuity between the core wire and the surrounding medium. However, this is not the case for the GaAs–$Al_xGa_{1-x}As$ system (the dielectric constant of $Al_xGa_{1-x}As$ is $13.18-3.12x$). Thus, they are safely to be ignored.

The multiple quantum wires can be produced by using the ''spacer'' process. Figure 1 shows the key steps in fabricating the multiple quantum wires. First of all, a GaAs substrate is used. Since the top layer is single crystalline, the quality of the wire made by this single crystalline can be maintained. The thickness of this top layer ranges from 30 to 200 nm. These wafers can be easily obtained from market. Based on the etching selectivity, a GaAs film around 150 nm in thickness (the thickness is related to the quantum wire length) is deposited in a low-pressure chemical vapor deposition, or LPCVD, system. After that, the GaAs film is patterned (e.g., a circular disk shape as shown in the Fig. 1) and etched. Then, a AlGaAs film can also be deposited in the LPCVD system. The thickness of this AlGaAs film is critical and must be uniform, ranging from 50 to 300 nm [Fig. 1(a)]. The etching selectivity between AlGaAs and bottom oxide is larger by using the state-of-the-art etcher. This means that we can control the processing time exactly and can prevent over etching the underlying oxide. After this etch-back process, a spacer is formed closely adjoining the AlGaAs pattern. If the pattern of GaAs is a circle, the spacer at this step will look like a ring [Fig. 1(b)]. It is noted that width of this ring, ΔL, is around 0.5–0.6 of the deposited thickness of GaAs. That is, the width of the ring is uncontrollable by the lithographic

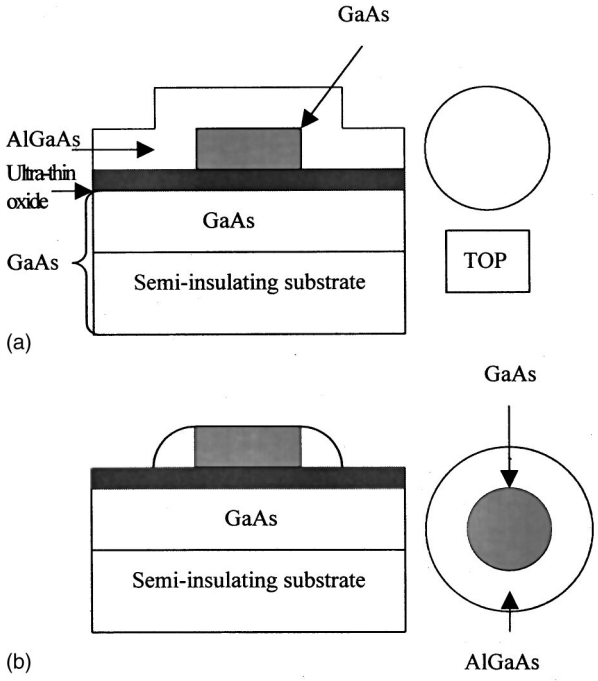

FIG. 1. Key steps in fabricating the multiple quantum wires with spacer process.

method, instead it depends on the thickness of the ring. Consequently, by controlling the thickness of the deposited AlGaAs, we can push the linewidth beyond the limitation of today's optical system. Thus, finally a two-layer quantum can be fabricated. This quantum wire is then masked and is deposited in a LPCVD of AlGaAs. Therefore, the outmost layer can be formed.

II. THEORY

The Hamiltonian of a hydrogenic impurity located off center in the multilayered quantum wire (MLQW) with a magnetic field is written as

$$H=-\frac{1}{2\mu}(\mathbf{P}+e\mathbf{A})^2-\frac{e^2}{\epsilon[(\boldsymbol{\rho}-\boldsymbol{\rho}_i)^2+\mathbf{z}^2]^{1/2}}+V(\rho), \quad (1)$$

where μ is the effective mass of the electron, ϵ is the dielectric constant of wire material, $\mathbf{A}$ is the magnetic-field vector potential, and V is the confining potential

$$V(\rho)=\begin{cases}0, & \text{if } \rho<a \quad (\text{GaAs})\\ V_2, & \text{if } a\leqslant\rho<b \quad (Al_xGa_{1-x}As)\\ V_3, & \text{if } \rho\geqslant b \quad (Al_yGa_{1-y}As)\end{cases}. \quad (2)$$

The $\boldsymbol{\rho}$ direction is perpendicular to the axis of the wire, $\boldsymbol{\rho}_i$ gives the location of the impurity along this direction, and $\mathbf{z}$ direction is along the axis of the wire. The MLQW system with $x>y$ (i.e., $V_2>V_3$) and $x<y$ (i.e., $V_2<V_3$) are indicated as MLQW-1 and MLQW-2, respectively. Where x and y are the Al concentration contained in the shell and the bulk regions of the MLQW system, respectively. Assuming the trial function of the eigenstate of the Hamiltonian in the absence of impurity is as the following form:

$$\Psi_1(\rho,\phi,z)=N_1M\left(\frac{1}{4}\alpha_1^2,\frac{m}{2},\lambda_1\rho^2\right)\Big/\sqrt{\lambda_1}e^{ikz}e^{im\phi}\quad\text{if}\quad\rho<a$$

$$\Psi_2(\rho,\phi,z)=\left[N_{21}M\left(\frac{1}{4}\alpha_2^2,\frac{m}{2},\lambda_2\rho^2\right)+N_{22}W\left(\frac{1}{4}\alpha_2^2,\frac{m}{2},\lambda_2\rho^2\right)\right]\Big/\sqrt{\lambda_2}e^{ikz}e^{im\phi}\quad\text{if}\quad a\leqslant\rho<b$$

$$\Psi_3(\rho,\phi,z)=N_3W\left(\frac{1}{4}\alpha_3^2,\frac{m}{2},\lambda_3\rho^2\right)\Big/\sqrt{\lambda_3}e^{ikz}e^{im\phi}\quad\text{if}\quad\rho\geqslant b, \tag{3}$$

where

$$\alpha_1^2=\left(\frac{2\mu E}{\hbar^2}-k^2-\frac{eBm}{\hbar}\right)\Big/\lambda_1\quad\lambda_1=\frac{eB}{2\hbar}$$

$$\alpha_2^2=-\left(\frac{2\mu(E-V_2)}{\hbar^2}-k^2-\frac{eBm}{\hbar}\right)\Big/\lambda_2\quad\lambda_2=\frac{eB}{2\hbar}$$

$$\alpha_3^2=-\left(\frac{2\mu(E-V_3)}{\hbar^2}-k^2-\frac{eBm}{\hbar}\right)\Big/\lambda_3\quad\lambda_3=\frac{eB}{2\hbar}, \tag{4}$$

and $M(\frac{1}{4}\alpha^2,m/2,\lambda\rho^2)$ and $W(\frac{1}{4}\alpha^2,m/2,\lambda\rho^2)$ are Whittaker function. Employing the continuity relation of wave functions at $\rho=a$ and $\rho=b$, one obtains the relations of N_1, N_{21}, N_{22}, and N_3:

$$N_1=\frac{N_{21}M\left(\frac{1}{4}\alpha_2^2,\frac{m}{2},\lambda_2a^2\right)+N_{22}W\left(\frac{1}{4}\alpha_2^2,\frac{m}{2},\lambda_2a^2\right)}{M\left(\frac{1}{4}\alpha_1^2,\frac{m}{2},\lambda_1a^2\right)}, \tag{5}$$

$$N_3=\frac{N_{21}M\left(\frac{1}{4}\alpha_2^2,\frac{m}{2},\lambda_2b^2\right)+N_{22}W\left(\frac{1}{4}\alpha_2^2,\frac{m}{2},\lambda_2b^2\right)}{W\left(\frac{1}{4}\alpha_3^2,\frac{m}{2},\lambda_3b^2\right)}. \tag{6}$$

If we set $N_{22}=N$ and $N_{21}=NN_2$, then the radial part of wave function becomes

$$R_1(\rho)=\frac{N_2M\left(\frac{1}{4}\alpha_2^2,\frac{m}{2},\lambda_2a^2\right)+W\left(\frac{1}{4}\alpha_2^2,\frac{m}{2},\lambda_2a^2\right)}{M\left(\frac{1}{4}\alpha_1^2,\frac{m}{2},\lambda_1a^2\right)}\times M\left(\frac{1}{4}\alpha_1^2,\frac{m}{2},\lambda_1\rho^2\right), \tag{7}$$

$$R_2(\rho)=N\left[N_2M\left(\frac{1}{4}\alpha_2^2,\frac{m}{2},\lambda_2\rho^2\right)+W\left(\frac{1}{4}\alpha_2^2,\frac{m}{2},\lambda_2\rho^2\right)\right], \tag{8}$$

$$R_3(\rho)=\frac{N_2M\left(\frac{1}{4}\alpha_2^2,\frac{m}{2},\lambda_2b^2\right)+W\left(\frac{1}{4}\alpha_2^2,\frac{m}{2},\lambda_2b^2\right)}{W\left(\frac{1}{4}\alpha_3^2,\frac{m}{2},\lambda_3b^2\right)}\times W\left(\frac{1}{4}\alpha_3^2,\frac{m}{2},\lambda_3\rho^2\right), \tag{9}$$

where N is the normalization constant. Furthermore, the requirement of the continuity of the derivative of the wave function at $\rho=a$, can be fulfilled if

$$N_2=\frac{W'\left(\frac{1}{4}\alpha_2^2,\frac{m}{2},\lambda_2a^2\right)M\left(\frac{1}{4}\alpha_1^2,\frac{m}{2},\lambda_1a^2\right)-W\left(\frac{1}{4}\alpha_2^2,\frac{m}{2},\lambda_2a^2\right)M'\left(\frac{1}{4}\alpha_1^2,\frac{m}{2},\lambda_1a^2\right)}{M\left(\frac{1}{4}\alpha_2^2,\frac{m}{2},\lambda_2a^2\right)M'\left(\frac{1}{4}\alpha_1^2,\frac{m}{2},\lambda_1a^2\right)-M'\left(\frac{1}{4}\alpha_2^2,\frac{m}{2},\lambda_2a^2\right)M\left(\frac{1}{4}\alpha_1^2,\frac{m}{2},\lambda_1a^2\right)}. \tag{10}$$

And, the trial function of the eigenstate of the impurity system can then be assumed as

$$\Psi_{i1}(\rho,\phi,z)=R_1(\rho)e^{-\lambda\sqrt{(\boldsymbol{\rho}-\boldsymbol{\rho}_i)^2+\mathbf{z}^2}}e^{ikz}e^{im\phi}/\sqrt{\lambda_1}, \tag{11}$$

$$\Psi_{i2}(\rho,\phi,z)=R_2(\rho)e^{-\lambda\sqrt{(\boldsymbol{\rho}-\boldsymbol{\rho}_i)^2+\mathbf{z}^2}}e^{ikz}e^{im\phi}/\sqrt{\lambda_2}, \tag{12}$$

$$\Psi_{i3}(\rho,\phi,z)=R_3(\rho)e^{-\lambda\sqrt{(\boldsymbol{\rho}-\boldsymbol{\rho}_i)^2+\mathbf{z}^2}}e^{ikz}e^{im\phi}/\sqrt{\lambda_3}, \tag{13}$$

where λ is the variational parameter. Using the boundary condition

$$\left.\frac{\partial\Psi_{i2}}{\partial\rho}\right|_{\rho=b}=\left.\frac{\partial\Psi_{i3}(\rho)}{\partial\rho}\right|_{\rho=b} \tag{14}$$

and

$$N^{-2}=-\pi\frac{d(G+H+M)}{d\lambda} \tag{15}$$

with

$$G=\int_0^a \rho R_1^2(\rho) I_0(2\lambda\rho_<) K_0(2\lambda\rho_>) d\rho, \tag{16}$$

$$H=\int_a^b \rho R_2^2(\rho) I_0(2\lambda\rho_<) K_0(2\lambda\rho_>) d\rho, \tag{17}$$

$$M=\int_b^\infty \rho R_3^2(\rho) I_0(2\lambda\rho_<) K_0(2\lambda\rho_>) d\rho, \tag{18}$$

where $\rho_<(\rho_>)$ is the smaller (larger) of ρ and ρ_i. The binding energy E_b of the hydrogenic impurity is defined conventionally as the energy difference between the energy of the system without the impurity and the energy of the system with the impurity; i.e.,

$$E_b=-\lambda^2-\frac{4(G+H+M)}{\dfrac{d(G+H+M)}{d\lambda}}. \tag{19}$$

In Eq. (19), the energy and length are expressed in Rydberg and Bohr radius of the wire material, respectively. For the single-layered quantum wire (SLQW) model, it is only to set $a=b$ and $V_2=V_3$.

III. RESULTS AND DISCUSSIONS

Figure 2 shows binding energy of a donor located at the center of SLQW for various magnetic fields $B=0$, 5, 10, and 20 T. And the Al concentration in the barrier materials is assumed to be $x=0.3(Al_{0.3}Ga_{0.7}As)$. For a SLQW with large wire radius in the absence of magnetic field (curve 1 in Fig. 2), the impurity behaves just like a three-dimensional free hydrogenic atom, thus its binding energy approaches 1 Ry. If the wire radius decreases, the confinement effect enhances the binding energy more prominently. Thus, the binding energy of the impurity increases monotonically with the wire radius. However, as the wire radius is further decreased, the state energy of the impurity may become higher than the confining barrier. In the meanwhile, the kinetic energy of the confined electron becomes larger by the uncertainty principle and thus increases the probability of the electron leaking outside the well. The electron behaves like a three-dimensional electron after a certain characteristic wire radius and is only weakly perturbed by the potential well. Therefore, the binding energy resumes 1 Ry again. From the curves shown in Fig. 2, one can note that the effect of applying the magnetic field is prominent for $a>1a_0^*$, it is clear that the influence of the magnetic field becomes diminished for $a<1a_0^*$. For $a<1a_0^*$, the geometrical or spatial localization overcomes the effect of the magnetic field. For a given value of magnetic field, the binding energy is larger than that without a magnetic field. The physical meaning of this is that increasing the strength of the magnetic field shrinks the electron wave function and decreases the cyclotron radius for the electron relative to the wire radius and confines the electron closer to the impurity. When the radius of SLQW in the range $a\leqslant 1.0a_0^*$, we may observed that the binding energy increases almost independently of the applied magnetic field. This enhancement observed in the binding energy is due to the fact that, as the wire radius reduces, the carrier wave function is compressed strongly inside the dominant spatial confinement. However, at a certain small value of the wire radius, it reaches a maximum and then decreases as the wire radius reduces to zero. In this region, the binding energy continues to be dominated by the geometric confinement but, due to the leakage of the wave function into the barrier, its value at $a=0a_0^*$ approaches a quantity which is determined by the Landau level in the bulk material contained in the exterior of SLQW ($Al_{0.3}Ga_{0.7}As$). Our result is in good agreement with those of Pacheco[40] and Branis.[41] Thus, our MLQW model can be simplified well to the SLQW model as we set $a=b$ and $V_2=V_3$.

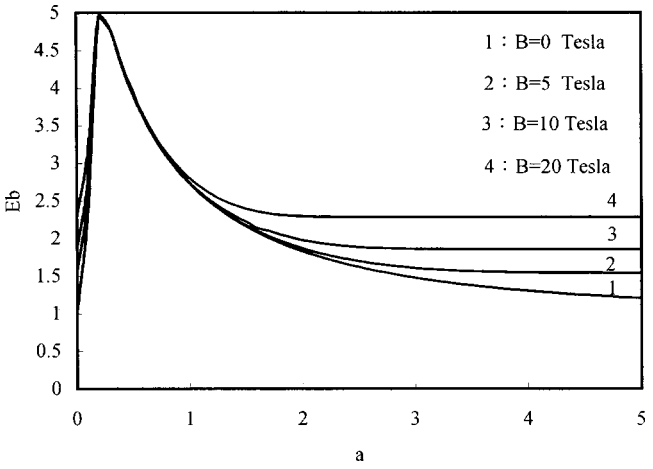

FIG. 2. Binding energy of donor in SLQW as a function of wire radius with $x=0.3$ ($Al_{0.3}Ga_{0.7}As$) for different magnetic fields $B=0$, 5, 10, and 20 T., respectively.

Figure 3 shows the binding energy of MLQW-1 as a function of core wire radius for different shell thicknesses with $x=0.3$, $y=0.1$, and the magnetic field $B=10$ T. To make a comparison between the cases of curve 5 and curve 6 which are the binding energies in SLQW with $x=0.3$ and $x=0.1$, respectively, one can note that for large wire radius

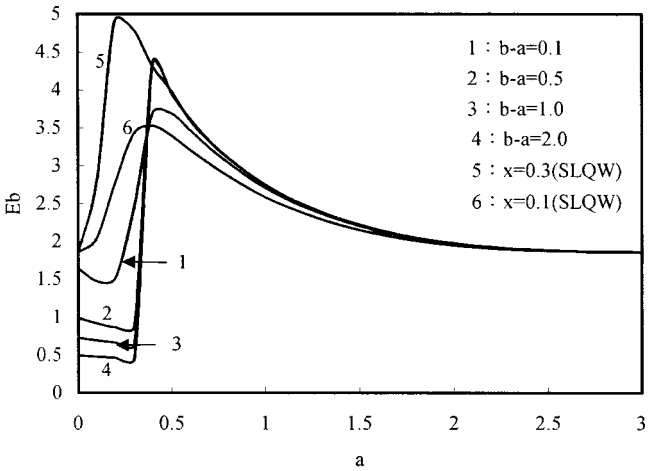

FIG. 3. Binding energy of donor in SLQW and MLQW-1 as a function of wire radius (or core wire radius) with magnetic field $B=10$ T. Curves 1, 2, 3, and 4 are the cases of MLQW-1 with $x=0.3$ and $y=0.1$ for different shell thicknesses $b-a=0.1$, 0.5, 1.0, and $2.0a_0^*$, respectively. For comparison, curves 5 and 6 are the cases in SLQW with $x=0.3$ and $x=0.1$, respectively.

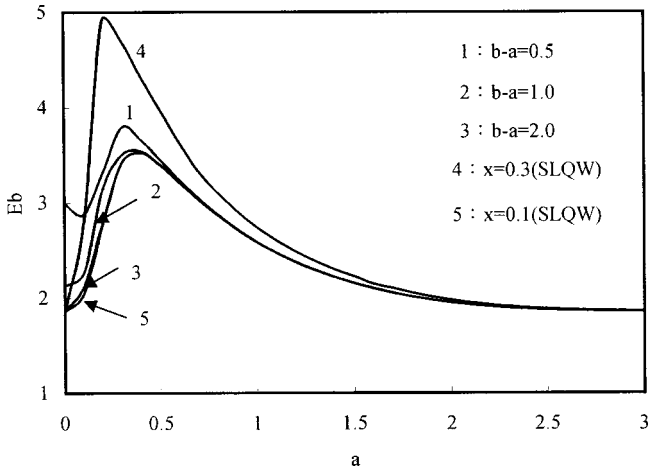

FIG. 4. Binding energy of donor in SLQW and MLQW-2 as a function of wire radius (or core wire radius) with magnetic field $B=10$ T. Curves 1, 2, and 3 are the cases of MLQW-2 with $x=0.1$ and $y=0.3$ for different shell thicknesses $b-a=0.5$, 1.0, and $2.0a_0^*$, respectively. For comparison, curves 4 and 5 are the cases in SLQW with $x=0.3$ and $x=0.1$, respectively.

the E_b is independent of the potential barrier height. And the E_b is influenced by the potential barrier height as the wire radius is reduced to a smaller value which is less than some characteristic value. In Fig. 3, we can see the E_b is independent of the potential barrier height for $a>2a_0^*$ and the E_b depends on the potential barrier height for $a<2a_0^*$ as expected. When we compare curves 1, 2, 3, and 4(MLQW-1 with $x=0.3$ and $y=0.1$) to curve 5(SLQW with $x=0.3$), one can see that as the potential barrier of the bulk region is lowered, the probability for an electron tunneling from the core region through the shell region and finally into the bulk region becomes larger as the core radius is decreased. Therefore, the binding energy of the impurity for the case with $V_2>V_3$ (i.e., MLQW-1) reduces prominently. Figure 4 shows the binding energy of the MLQW-2 as a function of core wire radius for different shell thicknesses with $x=0.1$, $y=0.3$, and the magnetic field $B=10$ T. The binding energy of MLQW-2 is almost uninfluenced by the Al concentration of bulk region material for $a>0.5a_0^*$, the curves 1, 2, 3, and

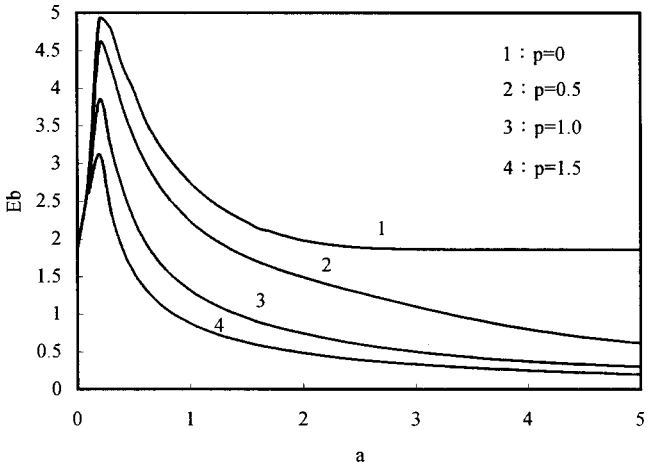

FIG. 6. Binding energy of donor in SLQW as a function of wire radius with magnetic field $B=10$ T and $x=0.3$ for different p ($p=\rho_i/a$).

5 almost overlap in this region. As the shell thickness increases the properties of the MLQW-2 ($x=0.1$ and $y=0.3$) is closer to that of SLQW ($x=0.1$). Curve 1 ($b-a=0.5a_0^*$) is different from the other curves. This is due to the fact that the thinner shell thickness increases the binding of the bulk potential barrier as the wire radius is decreased. Figure 5 shows the binding energy of the MLQW-1 as a function of magnetic field with $x=0.3$, $y=0.1$, and shell thickness $b-a=1a_0^*$ for various core wire radii $a=0.5$, 1.0, and $3.0a_0^*$, respectively. Curve 1 (for $a=0.5a_0^*$) and curve 2 (for $a=1.0a_0^*$) are independent of the applied magnetic field. And, curve 3 (for $a=3.0a_0^*$) shows that the E_b increases as the applied magnetic field is increased. The manner of E_b being influenced by the applied magnetic field in a MLQW is the same as that in a SLQW.

Figure 6 displays the binding energy of a SLQW as a function of wire radius for various p ($p=\rho_i/a$) with $x=0.3$ and $B=10$ T. As the donor approaches the wire boundary, the binding energy decreases due to the repulsion of the donor-electron wave function by the barrier potential. In Fig. 6, one can see that the binding energy decreases as the im-

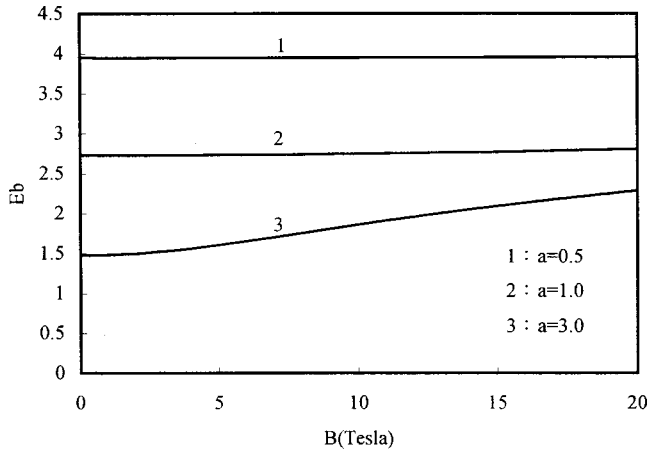

FIG. 5. Binding energy of donor in MLQW-1 as a function of magnetic field (B) with the shell thickness $b-a=1.0a_0^*$ for various core wire radii $a=0.5$, 1.0, and $3.0a_0^*$, respectively.

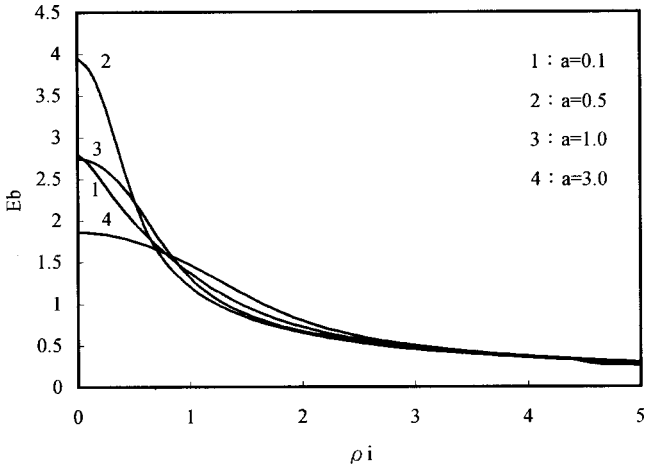

FIG. 7. Binding energy of donor in SLQW as a function of ρ_i with magnetic field $B=10$ T and $x=0.3$ for different wire radii $a=0.1$, 0.5, 1.0, and $3.0a_0^*$.

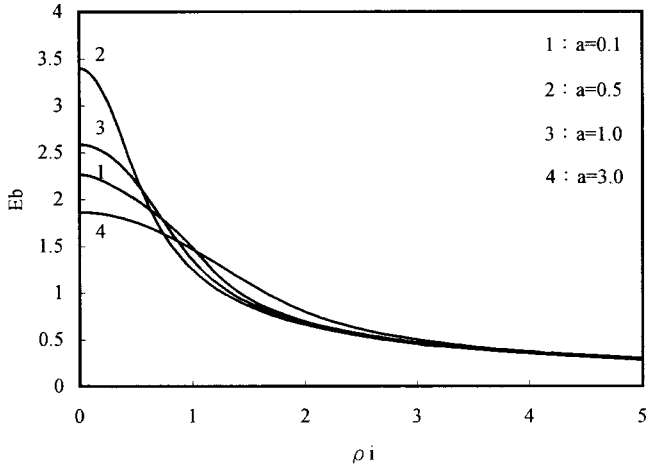

FIG. 8. Binding energy of donor in MLQW-2 ($x=0.1$ and $y=0.3$) as a function of position of impurity with $B=10$ T and the shell thickness $b-a=1a_0^*$ for various core wire radii $a=0.1$, 0.5, 1.0, and $3.0a_0^*$, respectively.

purity is moved away from the center in the SLQW as expected. The curve of E_b attains the maximum value at $a=0.2a_0^*$ and decreases as the wire radius is reduced. This decrease is due to the electron leaking out of the potential well. And we can see, the curves of E_b overlap each other as the electron leaking out of the potential well. This means that the E_b is independent of the position of impurity as the electron leaking out of the potential well. Figure 7 shows the binding energy of a donor in a SLQW as a function of position of impurity with $x=0.3$ and $B=10$ T for various wire radii. All of the curves decrease as the impurity is moved away from the center. Figures 8–9 show the binding energy in the MLQW-2 ($x=0.1$ and $y=0.3$) and MLQW-1($x=0.3$ and $y=0.1$) as a function of position of impurity with $B=10$ T and $b-a=1a_0^*$. Since no tunneling effect in MLQW-2 occurs, the feature of Fig. 8 behaves in a same manner as the SLQW does. For curve 1 ($a=0.1a_0^*$ and $b=1.1a_0^*$) in Fig. 9, the binding energy increases as the impurity is moved away from the center, and attains maximum value as $\rho_i \sim 1.8a_0^*$, it then decreases as the impurity is further moved away. This is due to the fact that the electron leaks out of the well and tunnels to the bulk region for $a=0.1a_0^*$. The Coulomb interaction increases and the magnetic field keeps the electron closer to the shell barrier and thus increases the repulsion of the electron by the shell barrier as the impurity is moved away from the center. This makes the binding energy increase. Furthermore, the binding energy decreases as ρ_i is increased. For curves 2, 3, and 4, since there are no tunneling effects for the core wire radius $a=0.5$, 1.0, and $3.0a_0^*$, the binding energies of the donor decrease as the impurity is moved away from the center, thus it is very similar to the case of SLQW.

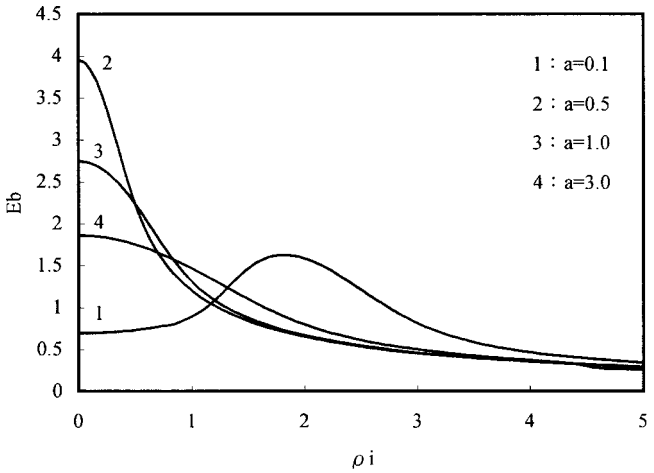

FIG. 9. Binding energy of donor in MLQW-1 ($x=0.3$ and $y=0.1$) as a function of position of impurity with $B=10$ T and the shell thickness $b-a=1a_0^*$ for various core wire radii $a=0.1$, 0.5, 1.0, and $3.0a_0^*$, respectively.

IV. CONCLUSION

In this article, we calculated the binding energy of donor impurity located at the center and off center of the SLQW, MLQW-1, and MLQW-2 in the presence of magnetic field. Our MLQW model could be simplified to SLQW and the results are found to be in good agreement with the results of other authors. Our calculation shows that the binding energy depends on the potential profiles, potential barrier height, impurity position, shell thickness, magnetic field, and the difference between the Al concentrations contained in the shell and bulk regions. And, we can see the electron tunnels to the bulk region as the core wire radius is reduced to a value which is smaller than the characteristic radius in the MLQW-1 model. In such a case, the behavior of the electron is very different from the other situation.

One possible benefit from our result is that these multiple quantum wires can be used to study the electron transport effect in quantum structure systems. If one deposits the source and drain on the ends of the quantum wires, then due to the tunneling effect between different layers, the electron transport phenomena will be very different from the case of the SLQW. One can also study the behavior of the electron conductivity as the source is connected to one layer while the drain is connected to the other layer. An additional interesting feature of the conductivity can be expected for the multiple quantum wire systems when the multiple quantum wire is put between two metal gates which can input time varying fields (E or B fields). With this kind of device, it is hopefully expected that the multiple quantum wires might have possible applications in the few-electron detectors in the future.

ACKNOWLEDGMENTS

The author acknowledges helpful discussions with Professor Der-San Chuu, Department of Electrophysics, National Chiao-Tung University, Hsinchu, Taiwan. This work is supported by Deh Yu College of Nursing and Management, Taiwan, Republic of China.

[1] G. Bastard, Phys. Rev. B **24**, 4714 (1981).
[2] J. W. Brown and H. N. Spector, J. Appl. Phys. **59**, 1179 (1986).
[3] N. P. Montenegro, J. Lòpez-Gondar, and L. E. Oliveira, Phys. Rev. B **43**, 1824 (1991).
[4] W. T. Masselink, Y. C. Chang, and H. Morkoc, Phys. Rev. B **28**, 7373 (1983).

[5] G. W. Bryant, Phys. Rev. B **31**, 7812 (1985).
[6] G. W. Bryant, Phys. Rev. B **29**, 6632 (1984).
[7] R. C. Miller, A. C. Gossard, W. T. Tsang, and O. Munteanu, Phys. Rev. B **25**, 3871 (1982).
[8] A. Latgé, M. de Dios-Leyve, and Luiz E. Oliveira, Phys. Rev. B **49**, 10450 (1994).
[9] X. Liu, A. Petrou, and B. D. McCombe, Phys. Rev. B **38**, 8522 (1982).
[10] D. S. Chuu, C. M. Hsiao, and W. N. Mei, Phys. Rev. B **46**, 3898 (1992).
[11] C. M. Hsiao, W. N. Mei, and D. S. Chuu, Solid State Commun. **81**, 807 (1992).
[12] S. V. Nair, L. M. Ramaniah, and K. C. Rustagi, Phys. Rev. B **45**, 5969 (1992).
[13] G. T. Einevoll and Y. C. Chang, Phys. Rev. B **40**, 9683 (1989).
[14] A. Kumar, S. E. Laux, and F. Stern, Phys. Rev. B **42**, 5166 (1990).
[15] N. Porras-Montenegro and S. T. P. Merchancano, Phys. Rev. B **46**, 9780 (1992).
[16] J. L. Zhu, J. H. Zhao, W. H. Duan, and B. L. Gu, Phys. Rev. B **46**, 7546 (1992).
[17] J. L. Zhu, J. J. Xiong, and B. L. Gu, Phys. Rev. B **41**, 6001 (1990).
[18] J. L. Zhu and X. Chen, Phys. Rev. B **50**, 4497 (1994).
[19] X. F. He, Phys. Rev. B **43**, 2063 (1991).
[20] T. Arakawa, M. Nishioka, Y. Ngamune, and Y. Arakawa, Appl. Phys. Lett. **64**, 2200 (1994).
[21] N. S. Mansour, Y. M. Sireko, K. W. Kim, and M. A. Littlejohn, Appl. Phys. Lett. **69**, 360 (1996).
[22] K. Kash, A. Scherer, J. M. Worlock, H. G. Graighead, and M. C. Tamargo, Appl. Phys. Lett. **49**, 1043 (1986).
[23] B. J. Skromme, R. Bhat, and M. A. Koza, Solid State Commun. **66**, 543 (1988).
[24] H. Temkin, G. J. Dolan, M. B. Panish, and S. N. G. Chu, Appl. Phys. Lett. **50**, 413 (1987).
[25] B. V. Shanabrook, J. Comas, T. A. Perry, and R. Merlin, Phys. Rev. B **29**, 7096 (1984).
[26] D. Gammon, R. Merlin, W. T. Maselink, and H. Morkoc, Phys. Rev. B **33**, 2919 (1986).
[27] V. Narayamurti, Phys. Today **37**, 24 (1984).
[28] S. Chaudhuri, Phys. Rev. B **28**, 4480 (1983).
[29] P. Lane and R. L. Greene, Phys. Rev. B **33**, 5871 (1986).
[30] D. Schooss, A. Mews, A. Eychmüller, and H. Weller, Phys. Rev. B **49**, 17072 (1994).
[31] A. Eychüller, A. Mews, and H. Weller, Chem. Phys. Lett. **208**, 59 (1993).
[32] A. Mews, A. Eychüller, M. Giersig, D. Schooss, and H. Weller, J. Phys. Chem. **98**, 934 (1994).
[33] A. Mews, A. V. Kadavaich, U. Banin, and A. P. Alivisatos, Phys. Rev. B **53**, R13242 (1996).
[34] J. Kido, K. Hongawa, K. Okuyama, and K. Nagai, Appl. Phys. Lett. **63**, 2627 (1993).
[35] B. Hu, Z. Yang, and F. E. Karasz, J. Appl. Phys. **76**, 2419 (1994).
[36] B. O. Dabbousi, M. G. Bawendi, O. Onitsuka, and M. F. Rubner, Appl. Phys. Lett. **66**, 1316 (1995).
[37] C. Y. Hsieh, Chin. J. Phys. (Taipei) **38**, 478 (2000).
[38] C. Y. Hsieh and D. S. Chuu, J. Phys.: Condens. Matter **12**, 8641 (2000).
[39] C. Y. Hsieh and D. S. Chuu, J. Appl. Phys. **89**, 2241 (2001).
[40] C. Y. Hsieh, J. Appl. Phys. **91**, 2326 (2002).
[41] M. Pacheco, Z. Barticevic, and A. Latgé, Physica B **302**, 78 (2001).
[42] S. V. Branis, G. Li, and K. K. Bajaj, Phys. Rev. B **47**, 1316 (1993).
[43] Y. X. Li, J. J. Liu, and X. J. Kong, J. Appl. Phys. **88**, 2588 (2000).
[44] G. Li, S. V. Brains, and K. K. Bajaj, Phys. Rev. B **47**, 15735 (1993).
[45] P. D. Wang, J. L. Merz, S. Fafard, R. Leon, D. Leonard, G. Medeiros-Ribeiro, M. Oestreich, P. M. Petroff, K. Uchida, N. Miura, H. Akiyama, and H. Sakaki, Phys. Rev. B **53**, 16458 (1996).
[46] R. Charrour, M. Bouhassoune, M. Fliyou, and A. Nougaoui, Physica B **293**, 137 (2000).
[47] A. A. Avetisyan, A. P. Djotyan, E. M. Kazaryan, and B. G. Poghosyan, Phys. Status Solidi B **225**, 423 (2001).
[48] E. Reyes-Gomez, A. Matos-Abiague, C. A. Perdomo-Leiva, M. de Dios-Leyva, and L. E. Oliveira, Phys. Rev. B **61**, 13104 (2000).
[49] S. T. Pérez-Merchancano and G. E. Marques, Solid State Commun. **110**, 209 (1999).
[50] E. Niculescu, A. Gearba, G. Cone, and C. Negutu, Superlattices Microstruct. **29**, 319 (2001).
[51] W. Xie, Phys. Lett. A **270**, 343 (2000).
[52] S. Chaudhuri and K. K. Bajaj, Solid State Commun. **52**, 967 (1984).
[53] R. L. Greene and K. K. Bajaj, Phys. Rev. B **31**, 913 (1985).
[54] B. Dong and Y. T. Wang, Solid State Commun. **89**, 13 (1994).
[55] P. Hawrylak and M. Grabowski, Phys. Rev. B **49**, 8174 (1993).
[56] Z. Xiao, J. Zhu, and F. He, J. Appl. Phys. **79**, 9181 (1996).
[57] S. Adachi, J. Appl. Phys. **58**, R1 (1985).